Period Doubling of a Torus in a Chain of Oscillators

Jean-Marc Flesselles,[1,2] Vincent Croquette,[2] and Stéphane Jucquois[2]
[1]*Institute Non Linéaire de Nice, Centre National de la Recherche Scientifique, 1361 route des Lucioles, 06560 Valbonne, France*
[2]*Laboratoire de Physique Statistique, École Normale Superiéure, Centre National de la Recherche Scientifique, 24 rue Lhomond, 75231 Paris Cedex 05, France*
(Received 12 March 1993)

We have experimentally studied the transition to chaos in a quasi-one-dimensional chain of nonlinear coupled oscillators, with periodic boundary conditions. We show that as long as the dynamics are not chaotic, this transition follows an unusual scenario: the period doubling of a T^2 torus. During this scenario all oscillators remain in phase. When the chain of oscillators bifurcates to chaos, it loses its spatial homogeneity and localized wave holes randomly propagate along the chain.

PACS numbers: 47.52.+j

After the understanding of chaotic behavior in nonlinear systems having a small number of degrees of freedom, interest has turned towards systems with spatial degrees of freedom. In particular, the problem of a 1D chain of nonlinear oscillators has received active attention. So far, a mechanism called spatiotemporal intermittency (STI) of spreading of chaotic patches has been pointed out [1,2] but no generic scenario of transition to chaos has been found in these systems. Finding spatially coherent structures in a temporally chaotic system also remains an open question [3].

In this work, we have performed accurate space-time measurements of an annular array of convective oscillators. We have focused on the transition from periodic to chaotic dynamics. We report on two phenomena. First, transition to chaos occurs via a subharmonic bifurcation of a two torus (T^2) [4]. Second, the chaotic regime involves localized objects related to Nozaki-Bekki holes [5]. To conclude we discuss the relevance of our experimental observations to general one-dimensional nonlinear systems.

We present here a Rayleigh-Bénard convection experiment in a low Prandtl number fluid (argon gas) in an annular geometry. As well understood since Busse [6], convection rolls of a low Prandtl number fluid undergo a bifurcation toward an oscillating state when driven beyond the convection threshold. Given the aspect ratio of the straight section of our cell, the convection pattern might be seen as a nearly one-dimensional chain of coupled nonlinear oscillators, with periodic boundary conditions.

The setup used here is very similar to the one used in a previous experiment [7], apart from the absence of lateral heating wires. The convection container has an annular shape, with an outer diameter of 40 mm, an inner diameter of 30 mm, and a thickness of 1.4 mm, giving an aspect ratio $\Gamma_\perp = 3.57$. It is filled with pressurized argon at 60 atm.

The cell is heated from below through a regulated copper block and its upper sapphire surface is maintained at fixed temperature with circulating water. The nondimensional control parameter is the Rayleigh number, $\mathrm{Ra} = g\alpha\Delta T d^3/\nu\kappa$ where g is the acceleration of gravitation, α is the thermal expansion coefficient, ΔT is the temperature difference between the top and bottom plates, ν and κ are the kinematic viscosity and the thermal diffusivity, and d is the thickness. At 60 atm, $\mathrm{Pr} = \nu/\kappa \simeq 0.72$ for Ar. We achieve a ΔT ranging from 0 to 40 K. Onset of convection occurs at $\Delta T \simeq 2$ K (or $\mathrm{Ra}_c \simeq 2000$) and onset of oscillatory instability at $\mathrm{Ra} \simeq 4\mathrm{Ra}_c$. Uncertainty of these measurements comes from the difficulty of detecting the onset of the convection bifurcation, but not from the temperature stability or accuracy (± 2 mK).

Convection gives rise to a pattern of 24 to 30 pairs of radial rolls, visualized by shadowgraphy (see Fig. 1). Flows of fluid at different temperatures appear with different gray levels.

Data acquisition is provided by a video camera con-

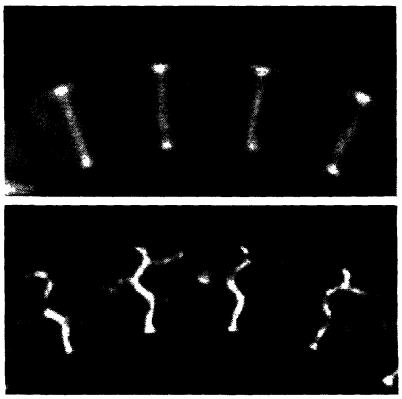

FIG. 1. Snapshots of part of the annular convective pattern (4 or 5 wavelengths out of 26). Top: stationary radial convective rolls. Bottom: above the oscillatory instability threshold, waves propagate radially along the rolls.

0031-9007/94/72(18)/2871(4)$06.00

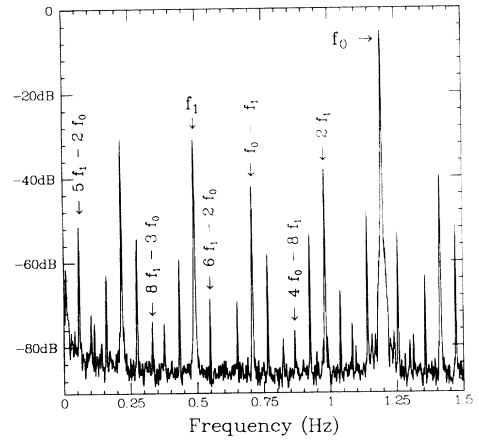

FIG. 2. Low frequency part of time spectrum in the biperiodic regime (26 pairs of rolls, $\Delta T = 20.49$ K). Here $f_1/f_0 = 0.409\,588$. Note the lowest frequency component $f_L = 5f_1 - 2f_0$.

nected to a frame grabber in a computer. Special care has been taken to reduce geometric distortions by synchronizing the camera such that pixels are actual squares. To analyze the temporal behavior of the pattern, 512 pixels regularly spaced on a circle, which intercept every roll of the pattern, are recorded at a frequency of 25 Hz, large enough for the 1 Hz oscillation frequency of the rolls. The recorded pixels are dumped to a hard disk for later processing. Series as long as 32 768 time steps (about 22 min) have been recorded, giving an absolute precision of 0.76 mHz from 0 to 12.5 Hz.

At each time step, the relevant information is the *positions of the rolls*. To extract this information, the data are spatially bandpassed and the Hilbert transform [8] is computed. This provides an imaginary part to the signal, whose phase gives the roll position. This way of measuring the position has the advantage of being normalized and independent of the light intensity. The dynamics are studied by temporal Fourier spectra of this phase signal. We have checked that these spectra have the same peak structure as spectra obtained from the raw video data.

At the threshold of the oscillatory instability, the oscillators can be prepared in two different states: either they all oscillate in phase or they do not. In the latter case they present a uniform phase shift from roll to roll such that the integrated phase is $2\pi n$, where n is found to be ± 1. In this Letter, we only consider the former case where all oscillators are in phase ($n = 0$) [9]. There, transition to chaos is well defined and exhibits features common to that observed in systems with a small number of degrees of freedom.

As a first approximation, the temporal Fourier power spectrum of the signal is independent of its position along the cell. As long as the oscillators are not chaotic, such spectra are made of sharp peaks originating from at most two frequencies and their harmonics. Figure 2 shows a typical example of such a spectrum. As the Rayleigh

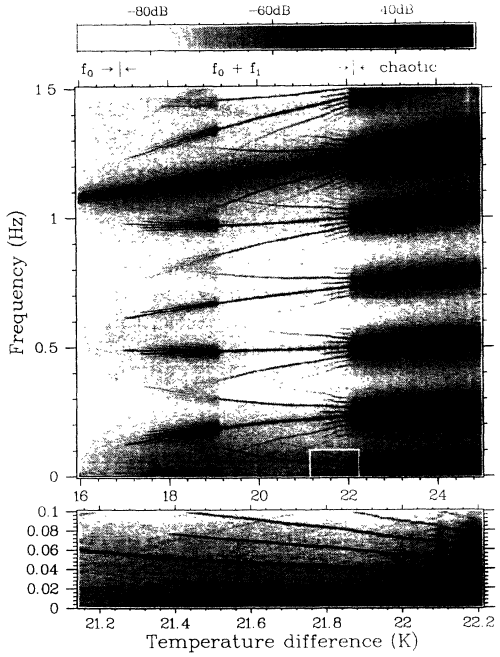

FIG. 3. Evolution of gray coded Fourier spectra as a function of ΔT for an increasing ramp (128 temperature steps) and 26 pairs of rolls. Spectra are monoperiodic for $\Delta T < 17.01$ K, chaotic for $\Delta T > 22.08$ K, and biperiodic in between. Nonhomogeneous biperiodism occurs for $17.37\text{ K} < \Delta T < 19.13$ K. The torus doubling takes place at $\Delta T = 21.38$ K. Lower part of the figure is a blowup of the white rectangle on 64 temperature steps.

number is varied, these spectra evolve. This evolution for an increasing temperature ramp is shown in Fig. 3, where, for each temperature step, the logarithm of the power is coded in gray level. The image for a decreasing ramp is very similar although fine details show small hysteresis.

Three regimes appear distinctly, with different spatiotemporal behavior. At low Ra (here $\Delta T \leq 17.01$ K) the system is monoperiodic with frequency f_0. At high Ra (here $\Delta T \geq 22.08$ K), it is chaotic. In between, it is (basically) biperiodic, with its secondary frequency f_1 being essentially temperature independent. Within the biperiodic domain, three different regimes are observed: close to the biperiodism threshold, frequency f_1 is not constant along the annulus but takes on two closely spaced values inside the cell (this leads to the "brushes" in Fig. 3). Above 19.13 K, f_1 recovers spatial homogeneity and biperiodism is pure. Moreover, in this regime all rolls oscillate in phase at all frequency components of the spectra. Finally above 21.38 K we observe the doubling of the T^2 torus as the scenario for the transition towards chaos.

In the temperature range where biperiodism is pure, all spikes in the temporal spectra may be labeled using only the two fundamental frequencies f_0 and f_1. The onset of the torus doubling occurs with the appearance of the subharmonic $f_L/2$ of the lowest frequency f_L of the spectrum

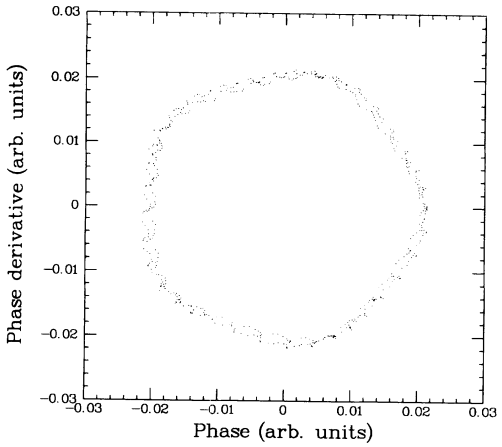

FIG. 4. Poincaré section at one spot in the cell showing the torus doubling. $\Delta T = 21.56$ K. Radius of torus in the other direction is of order 1. Here $f_1/f_0 = 0.405\,833$. The section presents a fivefold symmetry induced by the 2/5 locking; the fine modulations are related to the 13/32 nearby locking. Such sections are independent of the position in the cell.

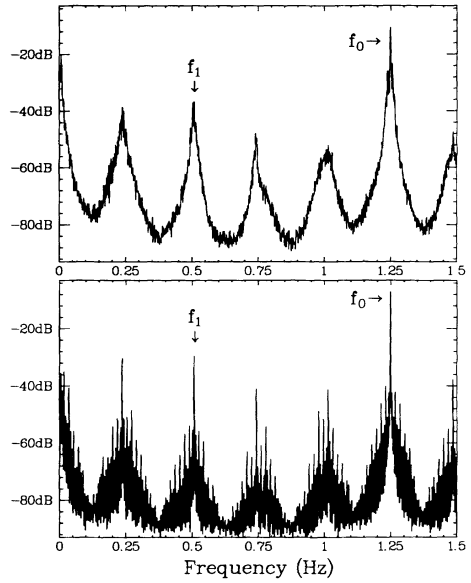

FIG. 5. Transition from biperiodic dynamics to chaotic dynamics. Bottom: biperiodic spectrum in the $f_L/6$ window ($\Delta T = 22.08$ K, $f_L/6 = 6.3$ mHz). Because of the small value of $f_L/6$, about 220 peaks are present. Top: chaotic spectrum obtained for $\Delta T = 22.09$ K. Note the five broad peaks.

(see blowup of Fig. 3). This frequency $f_L = 5f_1 - 2f_0$ is related to the nearby rational lock-in. The winding number $\Omega = f_1/f_0$ indeed decreases towards 2/5 while remaining slightly above it. Within experimental noise (90 dB) [10], no component $f_0/2$ nor $f_1/2$ is detectable. Also, in contrast with what is generally observed in two frequency systems [11], no frequency locking has been detected and the ratio f_1/f_0 evolves continuously with the Rayleigh number. Hence, the T^2 torus which represents the dynamical trajectory doubles at the bifurcation, as seen on the Poincaré section (Fig. 4). Further increase of Ra induces more subharmonic bifurcations followed by a chaotic window. In particular a bifurcation leading to $f_L/6$ (see Fig. 5) might precede the occurrence of $f_L/4$. The bifurcation cascade terminates after a few bifurcations and chaotic dynamics become the rule, sometimes disrupted by small windows of regular motion. Whenever the dynamics are regular, the oscillations are homogeneous in space; in contrast spatial homogeneity is lost within any chaotic window, however small.

The possibility of period doubling of a T^2 torus has been numerically explored by Kaneko [12] on mappings and numerically observed by Franceschini [13] on a system of differential equations arising from a seven-mode truncation of the Navier-Stokes equations. It has been studied from a mathematical point of view by Iooss and Los [4], and a physical approach has been given by Arnéodo, Coullet, and Spiegel [14]. The purpose of these studies was to determine whether a period-doubling cascade could be observed in a system with two incommensurate frequencies as typically occurs for a limit cycle [15,16]. To summarize the numerical and theoretical results, period doubling of a T^2 torus is possible in a wide range of parameters; however, small chaotic domains exist near each bifurcation point. It is thus expected that the cascade will abort after a few steps leading to the destruction of the T^2 torus.

To our knowledge, experimental observations of torus doubling have been reported in three different systems [17–19] but the whole scenario had not yet been observed; in particular, small chaotic domains were lacking. We present here the whole scenario for the first time.

As soon as the chain of oscillators undergoes chaotic dynamics, the signal obtained by a bandpass filter around f_1 displays spatially abrupt variations that we consider to be "wave holes." In the chaotic regime, the frequency peaks corresponding to the main and secondary frequencies have broadened but are still well defined. Since f_1 is close to a 2/5 subharmonic of f_0, and because of the chaotic enlarging of peaks, there are only five broad peaks in the relevant low frequency part of the spectrum, which allows for an unambiguous definition of the component of signal at f_0 or f_1 (see Fig. 5). The broadening of the peaks corresponds to some amplitude and phase modulations of the carrier frequencies f_0 and f_1; these modulations contain the actual informative signal. These frequencies correspond to the carrier frequencies and their broadenings to the modulations, which constitute the actual informative signal. Temporal filtering around f_0 or f_1 shows that, beside small phase fluctuations due to experimental imperfections of the cell, all oscillators remain in phase at f_0, whereas the signal associated with f_1 presents mobile localized defects. These defects are characterized by a strong amplitude dip and a phase jump localized at their cores. They typically travel over half a cell (see Fig. 6). The slower they move, the deeper

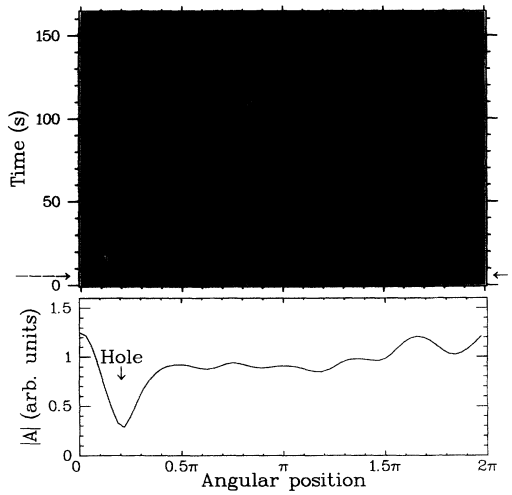

FIG. 6. Top: spatiotemporal evolution of holes in the f_1 component for a 26 roll pattern in the chaotic regime. Gray level is proportional to the local wave number. Medium gray represents homogeneous wave. Black and white correspond to phase jumps, hence to wave holes. Intense colors denote a slow moving hole, dim ones a fast moving hole. Abrupt black to white changes mark the nucleation of a spatiotemporal dislocation. Bottom: amplitude profile at time 6 s, as indicated by arrows, showing the wave depression.

the amplitude dip. These defects appear and disappear spontaneously and their averaged number increases with the forcing parameter.

These objects are strongly reminiscent of the so-called Nozaki-Bekki holes [5] and of the related objects studied by Manneville and Chaté [20,21] on the Landau-Ginzburg equation. They have already been observed by Janiaud *et al.* [22] in a nonhomogeneous pattern. In the present experiment, this localized wave defect emerges with the chaotic dynamics on a homogeneous pattern.

Our experiment exemplifies the route to chaos via a cascade of period doubling of a T^2 torus and illustrates the small chaotic domains surrounding its bifurcations. Using accurate spectrum analysis we have shown all the details of the predicted scenario. Moreover, we demonstrate that a chain of oscillators may transit towards spatiotemporal chaos by following a scenario typical of systems with a small number of degrees of freedom. However, we show that as soon as the dynamics becomes chaotic, the spatial degrees of freedom unfreeze through the appearance of localized defects of the Nozaki-Bekki type, thus providing new reasons to consider these types of defects among the elementary objects for the study of spatiotemporal chaos.

We thank A. Arnéodo, D. Bensimon, C. Bouchiat, A. Chenciner, A. Chiffaudel, G. Iooss, B. Janiaud, Y. Pomeau, and L. Tuckerman for enlightening discussions.

[1] F. Daviaud *et al.*, Physica (Amsterdam) **55D**, 287 (1992).
[2] M. Caponeri and S. Ciliberto, Physica (Amsterdam) **58D**, 365 (1992).
[3] I. Aranson, D. Golomb, and H. Sompolinsky, Phys. Rev. Lett. **68**, 3495 (1992).
[4] G. Iooss and J. Los, Commun. Math. Phys. **119**, 453 (1988).
[5] N. Bekki and K. Nozaki, Phys. Lett. **110A**, 133 (1985).
[6] F. Busse, J. Fluid Mech. **52**, 97 (1972).
[7] J. Lega, B. Janiaud, S. Jucquois, and V. Croquette, Phys. Rev. A **45**, 5596 (1992).
[8] A. V. Oppenheim and R. W. Schafer, *Digital Signal Processing* (Prentice-Hall, Englewood Cliffs, NJ, 1975).
[9] When $n \neq 0$, the pattern spins continuously inside the cell and chaos occurs at lower Ra. A detailed analysis will be given in a forthcoming paper.
[10] An estimate of this S/N ratio obtained with an 8-bit video board and the long time series is $S/N \approx 256 \times \sqrt{16384}$.
[11] J. A. Glazier and A. Libchaber, IEEE Trans. Circ. Syst. **35**, 790 (1988).
[12] K. Kaneko, Prog. Theor. Phys. **69**, 1806 (1983).
[13] V. Franceschini, Physica (Amsterdam) **D6**, 285 (1983).
[14] A. Arnéodo, P. H. Coullet, and E. Spiegel, Phys. Lett. **94A**, 1 (1983).
[15] M. Feigenbaum, J. Stat. Phys. **19**, 25 (1978).
[16] C. Tresser and P. Coullet, C.R. Acad. Sci. A **287**, 577 (1978).
[17] M. Basset and J. Hudson, Physica (Amsterdam) **35D**, 289 (1989).
[18] K. McKell, D. Broomhead, R. Jones, and D. Hurle, Europhys. Lett. **12**, 513 (1990).
[19] H. Haucke, Y. Maeno, and J. Wheatley, in *LT-17, Proceedings of the Seventeenth International Conference on Low Temperature Physics*, edited by U. Eckern, A. Schmid, W. Weber, and H. Wühl (Elsevier, Karlsruhe, Germany, 1984), pp. 1123–1124.
[20] H. Chaté and P. Manneville, Phys. Lett. A **171**, 183 (1992).
[21] H. Chaté, Nonlinearity **7**, 219, (1994).
[22] B. Janiaud, S. Jucquois, J. Lega, and V. Croquette, in *Pattern Formation in Complex Dissipative Systems*, edited by S. Kai (World Scientific, Kitakyushu, Japan, 1991), pp. 538–550.

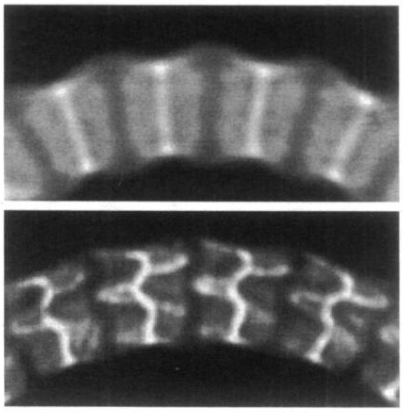

FIG. 1. Snapshots of part of the annular convective pattern (4 or 5 wavelengths out of 26). Top: stationary radial convective rolls. Bottom: above the oscillatory instability threshold, waves propagate radially along the rolls.

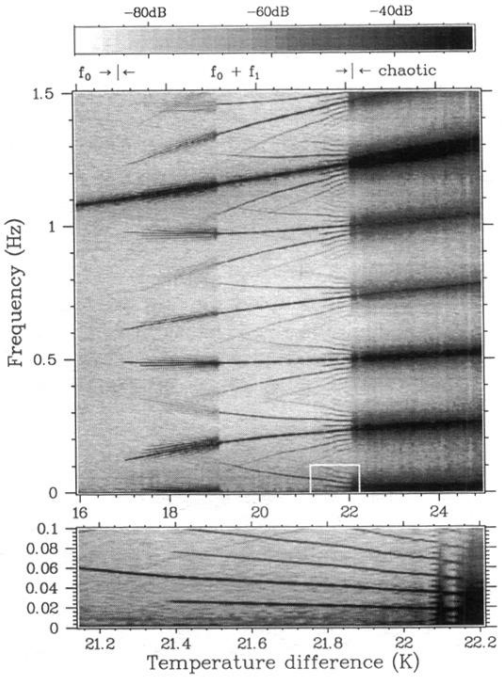

FIG. 3. Evolution of gray coded Fourier spectra as a function of ΔT for an increasing ramp (128 temperature steps) and 26 pairs of rolls. Spectra are monoperiodic for $\Delta T < 17.01$ K, chaotic for $\Delta T > 22.08$ K, and biperiodic in between. Nonhomogeneous biperiodism occurs for $17.37 \text{ K} < \Delta T < 19.13$ K. The torus doubling takes place at $\Delta T = 21.38$ K. Lower part of the figure is a blowup of the white rectangle on 64 temperature steps.

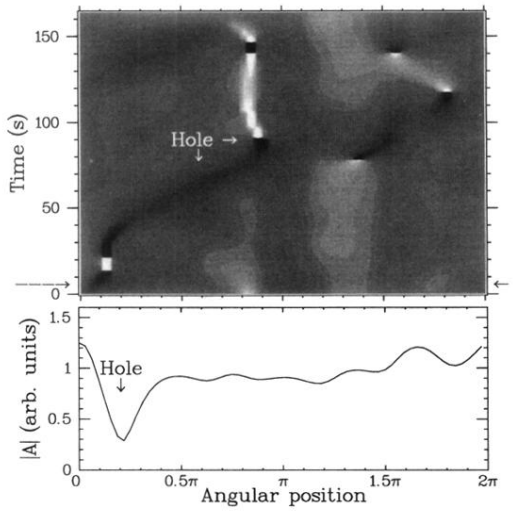

FIG. 6. Top: spatiotemporal evolution of holes in the f_1 component for a 26 roll pattern in the chaotic regime. Gray level is proportional to the local wave number. Medium gray represents homogeneous wave. Black and white correspond to phase jumps, hence to wave holes. Intense colors denote a slow moving hole, dim ones a fast moving hole. Abrupt black to white changes mark the nucleation of a spatiotemporal dislocation. Bottom: amplitude profile at time 6 s, as indicated by arrows, showing the wave depression.